RADIATIVE RECOMBINATION AND PHOTOIONIZATION PROCESSES INVOLVING HEAVY ELEMENT IMPURITIES IN PLASMA

M. B. Trzhaskovskaya
Department of Theoretical Physics
Petersburg Nuclear Physics Institute
Gatchina 188300, Russia

Research Co-ordination Meeting

on CRP

"Atomic data for heavy element impurities in fusion reactors"

14–15 November, 2005, IAEA, Austria

1 Project goals

In fusion research the impurities play an important role for the plasma modelling and diagnostics. The rate equations governing the ion–atom distributions involve data for the Radiative Recombination (RR) and photoionization processes. In RR, an electron is captured into the ground and excited states of the impurity ion and a photon is emitted simultaneously. The radiation contains an information on the plasma regimes which can be used to measure the plasma parameters (*e.g.* the temperature of the electron distribution).

The aim of our project is to produce new unified cross-section database for RR and photoionization processes as a function of electron energy for the impurity atomic charge states from neutral to highly charged ions. We intend to consider primarily the heavy element impurities like W, Mo and then Ar, Kr, Xe, Fe, Cu and others. The calculations will be carried out by the self-consistent Dirac–Fock method. All essential multipole orders of the photon field will be taken into account. Relativistic and retardation effects become severe for heavy and highly charged ions as well as at high photon energies while the majority of previous results were obtained using the nonrelativistic Hartree–Fock method. The calculated subshell RR cross sections as well as RR rate coefficients will be fitted by simple analytic expressions in a wide photon/electron energy range. The fit parameters for heavy impurities important to the present CRP will be tabulated.

2 Scientific background

The RR cross sections and rate coefficients are obtained by the principle of detailed balance from Photoionization Cross Section (PCS). A number of systematic tabulations of PCS are available to date but almost all for the ground state of atoms except a few:

(i) Opacity Project by Seaton (1987) [1] and by Fernley *et al.* (1999) [2] which entails extensive nonrelativistic Hartree–Fock calculations of PCS for ground and low excited states of atoms or ions. Under the project, PCS of a large number of atoms and ions, primarily of astrophysical abundant elements have been computed.

(ii) Clark *et al.* (1986) [3] performed Hartree–Fock calculations of configuration averaged PCS for ground and excited states $1s \leq nl \leq 5\,g$ in He-like through Al-like iso-electronic sequences of atoms ionized four or more times with $6 \leq Z \leq 100$. The PCS were fitted by the analytic expression involving 15 fit parameters as a function of the atomic number Z in the photon energy range between the ionization threshold ε and 10ε with average error less than 10% (a maximum error is between 10% and 50%).

(iii) Relativistic benchmark calculations of subshell cross sections for RR of an electron with bare nuclei were performed by Ichihara and Eichler (2000) [4].

(iv) The unified scheme using the R-matrix method was used for electron-ion recombination by Nahar *et al.* (2004) [5] with allowance made for relativistic effects.

Our previous studies in this field are concerned with the following points.

(i) Precise relativistic calculations of total and differential cross sections of RR of an electron with the H-, He-, and Li-like uranium ions were carried out by Nikulin and Trzhaskovskaya (2003) in the framework of the Dirac–Fock method with regard to the contribution of the Breit electron interaction and the main quantum electrodynamic corrections [6]. The subshell cross sections were calculated with an accuracy of 0.1%. The calculational accuracy was verified by comparison of our results for RR of an electron with a bare nucleus with benchmark calculations by Ichihara and Eichler (2000) [4]. Our calculations of the angular distribution of unpolarized photons emitted in the case of a capture of electrons into the K and L shells of the uranium ions listed above are in good agreement with experimental data obtained at GSI (2000) [7].

(ii) PCS of atoms and ions from He to Zn for all subshells of ground state atoms and ions were calculated in our papers (1990, 1993) [8, 9] within the relativistic Dirac–Fock–Slater method for photon energies E between ε and 100ε. The PCS were fitted by simple analytic expressions containing five fit parameters for $E \leq 50\,\mathrm{keV}$ with the average error less than 2% (a maximum error is between 4% and 14%). The ionization energies ε were fitted by simple polynomials of atomic number Z and number of atomic electrons N. The fit parameters were tabulated and published in journal ADNDT [9].

(iii) Extensive tabulations of subshell and total PCS including the dipole parameters of the angular asymmetry for all elements with $Z \leq 100$ in the

photon energy range $0.13 - 4.5\,\mathrm{keV}$ were also presented in ADNDT (1979) [10]. Tabulations of PCS were based on the Dirac–Fock–Slater calculations.

(iv) The non-dipole parameters of photoelectron angular distribution were studied by us in the quadrupole approximation (2001, 2002) [11, 12], and in the octupole approximation (2004, 2005) [13, 14] as well as including all multipole orders of the photon field (2001) [15]. The nondipolar photoelectron angular distribution parameters for majority of shells of elements $1 \leq Z \leq 100$ in the photoelectron energy range $0.1 - 10\,\mathrm{keV}$ were published in ADNDT [11, 14].

3 Proposed methods and preliminary calculations

The main aim of our project is to provide new data for the radiative recombination of heavy impurities with electrons and, consequently, for the inverse process of photoionization, which are primarily required in plasma modeling (radiation power losses) and in plasma diagnostics, especially in the low-temperature edge region.

To achieve these goals, we plan first of all, to critically reassess the available data information for RR and photoionization processes with the aim to identify the specific heavy element impurity ions, for which data are of a prime necessity in the study of plasma modeling and in diagnostics. The fully relativistic calculations of the subshell and total RR cross sections will be performed for ground and excited states of the heavy element impurities from neutrals to highly charged ions. All essential multipole orders of the photon field will be taken into account. The calculations will be carried out by the self-consistent Dirac–Fock method.

We will use our package of computer codes RAINE – "Relativistic Atom. Interaction of electromagnetic radiation and Nucleus with atomic Electrons" [16]. The computer codes have been developed using modern methods of calculations of atomic structure and electromagnetic processes. Relativistic effects, configuration mixing, the Breit magnetic interaction, and the higher order quantum electrodynamic corrections can be taken into account.

We plan to fit the subshell RR cross sections as well as rate coefficients by simple analytic expressions in the wide energy range. The fit parameters for important to the present CRP heavy impurities will be tabulated.

The Dirac–Fock method is expected to be accurate for multicharged ions, for inner shells of neutral and low-ionized atoms, and also enough far from the thresholds of outer shells of neutral and low-ionized atoms. The method may give errors near the thresholds of outer shells of neutral and low-ionized atoms where correlation effects may be considerable. Our calculations of total

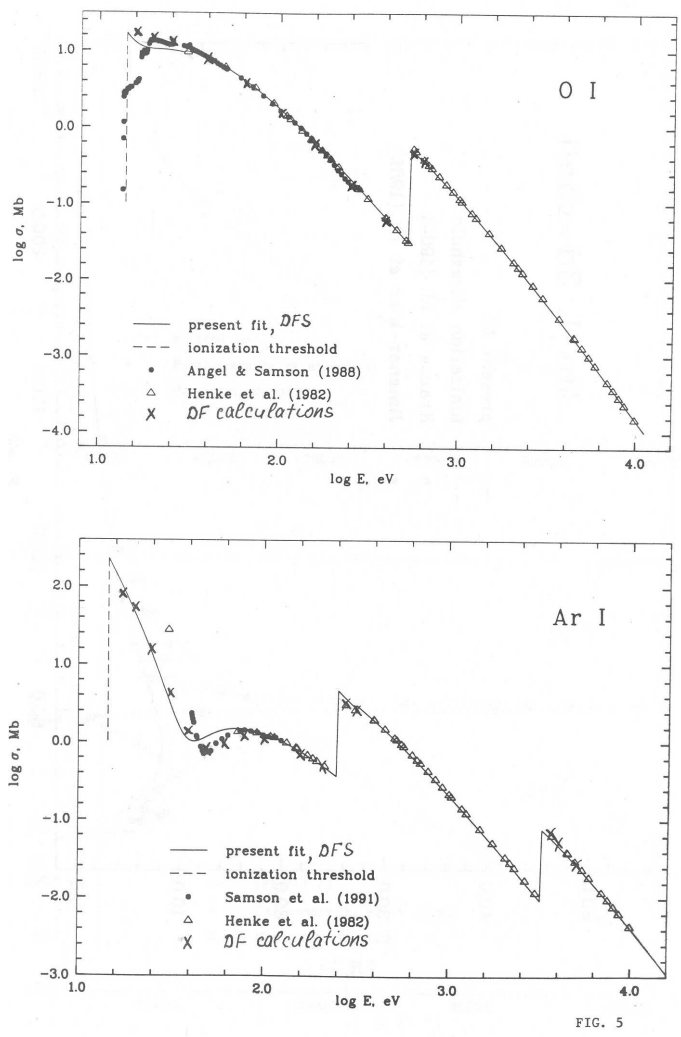

Figure 1: Total photoionization cross sections for neutral atoms O and Ar compared with experimental data by Angel and Sampson [17], Henke *et al.* [19], and Sampson *et al.* [18]. Solid curves, Dirac–Fock–Slater calculations, crosses, Dirac–Fock calculations.

PCS for neutral atoms of $Z = 8$ and $Z = 18$ are compared with experimental data in Fig. 1. Solid curves are related to the PCS calculations by the Dirac–Fock–Slater method with regard for the exchange interaction between electrons approximately. One can see that these calculations are in good agreement with experiment everywhere except energy ranges near ionization thresholds,

especially for thresholds of the most outer shells. Crosses are related to the Dirac–Fock calculations where the exchange is taken into account exactly. The crosses are marked mainly in the energy ranges near ionization thresholds where there is a discrepancy between Dirac–Fock–Slater calculations and experimental data. The Dirac–Fock method is shown to agree better with experiments in these ranges. As follows from Fig. 1, the Dirac–Fock results are quite adequate even for the most outer shells at the energy E above $\sim 40\,\mathrm{eV}$ the ionization threshold.

As an example of preliminary calculations, we considered the argon-like ion Fe^{8+}:[Ar]. The PCS σ_{ph} as well as cross sections of radiative recombination σ_{rr} of an electron with the ion at a capture of the electron into unfilled shells were calculated in the framework of the Dirac–Fock method.

I would remind the relevant expressions for RR cross sections and PCS in the relativistic case. The radiative recombination of an electron with an N-electron ion leads to formation of the $(N+1)$-electron ion. The subshell cross section $\sigma_{rr}^{(i)}$ of this process, accompanied by the capture of an electron to the i-th shell with quantum numbers $n\ell j$ can be expressed in terms of the corresponding photoionization cross section $\sigma_{ph}^{(i)}$ using the transfer coefficient which follows from the principle of detailed balance and in our case has the form

$$\sigma_{rr}^{(i)} \;=\; \frac{(2j_i+1)E^2}{2m_0c^2(E-\varepsilon_i)}\sigma_{ph}^{(i)}. \qquad (1)$$

For the case of unpolarized or circularly-polarized radiation, the relativistic PCS can be written as

$$\begin{aligned}\sigma_{ph}^{(i)} \;&=\; \frac{4\pi^2\alpha}{E}\sum_L\sum_\kappa\Big[(2L+1)Q^2_{L\,L}(\kappa)+LQ^2_{L+1\,L}(\kappa)\\ &+\; (L+1)Q^2_{L-1\,L}(\kappa)-2\sqrt{L(L+1)}Q_{L-1\,L}(\kappa)Q_{L+1\,L}(\kappa)\Big]. \qquad (2)\end{aligned}$$

In Eqs.(1) and (2), L is the multipolarity of the radiation field; $\kappa=(\ell-j)(2j+1)$ is the relativistic quantum number; ℓ and j are the total and orbital angular momenta of an electron; α is the fine structure constant; E is the photon energy; ε_i is the binding energy of the i-th shell. Eq.(2) and all equations below make use of relativistic units where $\hbar=m_0=c=1$.

The reduced matrix elements $Q_{\Lambda L}(\kappa)$ are determined by the expression

$$
\begin{aligned}
Q_{\Lambda L}(\kappa) &= ([\bar{\ell}][\ell_i]/[\Lambda])^{1/2} C^{\Lambda 0}_{\bar{\ell} 0 \ell_i 0}\, \mathcal{A} \begin{pmatrix} \bar{\ell} & 1/2 & j \\ \ell_i & 1/2 & j_i \\ \Lambda & 1 & L \end{pmatrix} R_{1\Lambda} \\
&+ ([\ell][\bar{\ell}_i]/[\Lambda])^{1/2} C^{\Lambda 0}_{\ell 0 \bar{\ell}_i 0}\, \mathcal{A} \begin{pmatrix} \ell & 1/2 & j \\ \bar{\ell}_A & 1/2 & j_i \\ \Lambda & 1 & L \end{pmatrix} R_{2\Lambda}\,, \qquad (3)
\end{aligned}
$$

where $\bar{\ell} = 2j - \ell$, $C^{\Lambda 0}_{\ell_1 0 \ell_2 0}$ is the Clebsch–Gordan coefficient, $\mathcal{A} \begin{pmatrix} \ell_1 & 1/2 & j_1 \\ \ell_2 & 1/2 & j_2 \\ \Lambda & 1 & L \end{pmatrix}$ is the recoupling coefficient for the four angular momenta, $[a]$ denotes the expression $(2a+1)$, $R_{1\Lambda}$ and $R_{2\Lambda}$ are the radial integrals in the form

$$
\begin{aligned}
R_{1\Lambda} &= \int_0^\infty G_i(r) F_\kappa(r) j_\Lambda(Er) dr\,, \\
R_{2\Lambda} &= \int_0^\infty G_\kappa(r) F_i(r) j_\Lambda(Er) dr\,. \qquad (4)
\end{aligned}
$$

Here $j_\Lambda(Er)$ is the spherical Bessel function of the Λ-*th* order, and $G(r)$ and $F(r)$ are the large and small components of the Dirac radial electron wave function. Subscripts i and κ are related to the bound and free electron, respectively.

Using Eqs. (1)–(4), we calculated cross sections of RR of an electron with the ion Fe^{8+}:[Ar] when the electron is captured into unfilled shells $n\ell j$ beginning from the $3d$ shells up to 15ℓ shells, or what is the same, of photoionization of the $n\ell j$ shells of the ion Fe^{7+}:[Ar]$n\ell j$. For a specific value of n, all possible values of the relativistic quantum number κ should be taken into account. The energy range under consideration is from 4 eV above the ionization threshold of the *i-th* shell, that is ε_i+4 eV, up to $100\varepsilon_i$. PCS for shells with $3 \le n \le 12$ in dependence on the photon energy E are presented in Fig. 2 for the $s_{1/2}$, $p_{1/2}$, $d_{3/2}$, and $f_{5/2}$ shells. Clearly that PCS per one electron for shells with the same orbital momenta ℓ for $Z = 26$ are rather close to each other.

All curves are very smooth with no minima and maxima because we consider the highly charged ion. Curves for shells with the same orbital quantum number ℓ are similar to each other in a shape, even if they have a slightly different slope approaching each other with increasing the energy E.

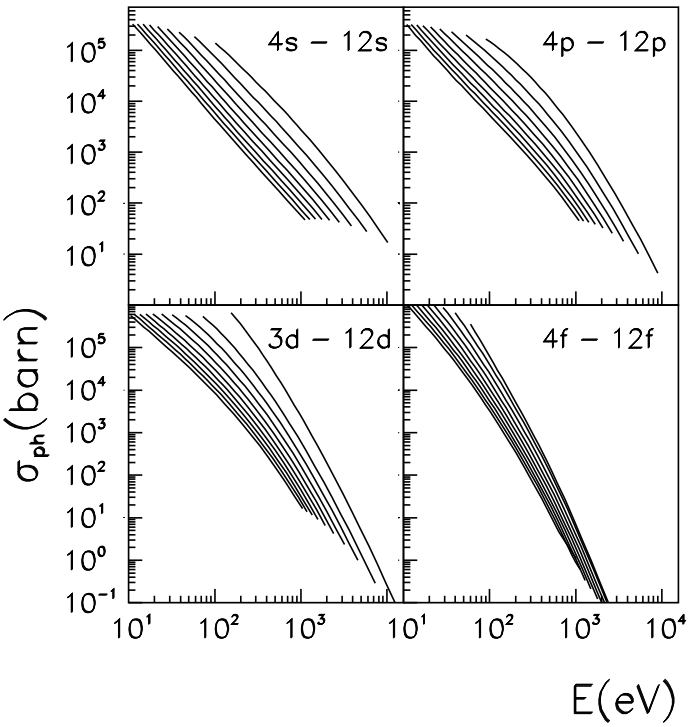

Figure 2: Photoionization cross sections σ_{ph} (barn) for electron states $n\ell j$ $(3 \leq n \leq 12)$ of the ion Fe^{7+}:[Ar]$n\ell j$ as a function of the photon energy E (eV)

Fig. 3 displays the E-dependence of the RR cross sections $\sigma_{rr}(E)$ for the same shells. These curves fall off more markedly in the energy range near the ionization threshold due to the factor in Eq. (1). Nevertheless, the curves $\sigma_{rr}(E)$ are also rather smooth for the ion under consideration.

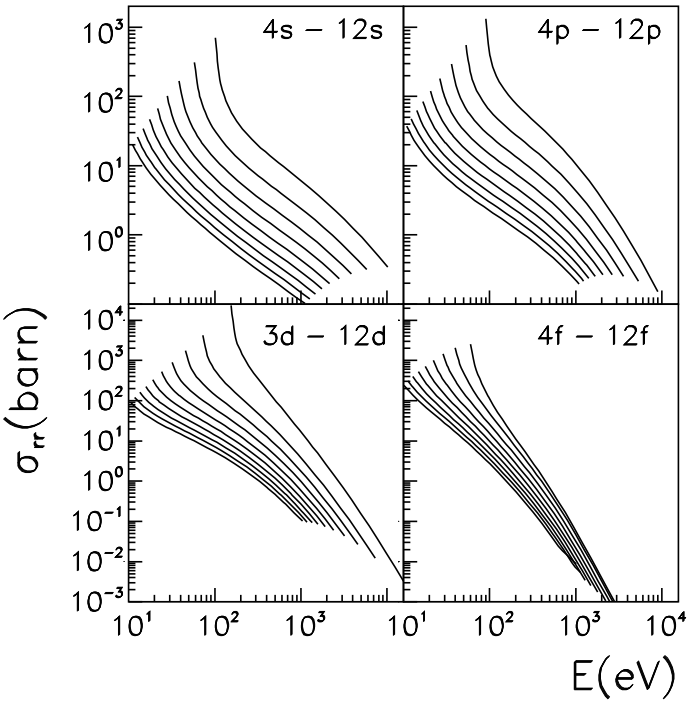

Figure 3: Radiative recombination cross sections σ_{rr} (barn) with capture of an electron into unfilled shells $n\ell j$ $(3 \le n \le 12)$ of the ion Fe^{8+}:[Ar] versus the photon energy E (eV)

Besides, we calculated the total RR cross sections $\sigma_{rr}^{(tot)}$ which is of great importance in plasma studies. Presented in Table 1 are contributions $\sigma_{rr}^{(n)}$ of shells with various values of principal quantum number n to the total RR cross section, $\sigma_{rr}^{(n)}$ being defined as follows

$$\sigma_{rr}^{(n)} \;=\; \sum_{\kappa} \sigma_{rr}^{(n\kappa)}. \qquad (5)$$

Note that $\sigma_{rr}^{(n\kappa)} \equiv \sigma_{rr}^{(i)}$. In the case of the ion Fe^{8+}, there are only two terms in Eq. (5) with $n = 3$ (the $3d$ shells) while for $n \ge 4$, the summation extends over $(2n-1)$ values of quantum number κ.

We notice that the contribution $\sigma_{rr}^{(n)}$ decreases with n. However there is no very rapid convergence in this case. Although the contributions for n=15 at energies under consideration are small (of the order of tenths of a percent), we

Table 1: Partial RR cross sections $\sigma_{rr}^{(n)} = \sum_\kappa \sigma_{rr}^{(n\kappa)}$ (in barn) for ion Fe^{8+}:[Ar] and its contributions to the RR total cross section $\sigma_{rr}^{(tot)}$ $\Delta_n = (\sigma_{rr}^{(n)}/\sigma_{rr}^{(tot)}) \times 100\%$. $\bar{\sigma}_{rr}^{(tot)}$ is the total RR cross section with allowance made for the remainder estimated using the Kramers summation method.

	$E = 0.5\,\mathrm{keV}$		$E = 1\,\mathrm{keV}$		$E = 10\,\mathrm{keV}$	
n	$\sigma_{rr}^{(n)}$	$\Delta_n, \%$	$\sigma_{rr}^{(n)}$	$\Delta_n, \%$	$\sigma_{rr}^{(n)}$	$\Delta_n, \%$
3	174.5	50	28.1	32	0.0258	2.3
4	85.3	24	28.6	33	0.537	48
5	35.4	10	12.0	14	0.225	20
6	18.4	5.3	6.28	7.3	0.116	10
7	10.8	3.1	3.70	4.3	0.0676	6.1
8	6.91	2.0	2.36	2.7	0.0431	3.9
9	4.69	1.4	1.60	1.8	0.0289	2.6
10	3.33	1.0	1.14	1.3	0.0207	1.9
11	2.45	0.7	0.837	1.0	0.0152	1.4
12	1.85	0.5	0.665	0.8	0.0115	1.0
13	1.45	0.4	0.521	0.6	0.00878	0.8
14	1.26	0.3	0.402	0.5	0.00698	0.6
15	1.00	0.2	0.316	0.4	0.00560	0.5
$\sigma_{rr}^{(tot)}$	347.3		86.5		1.112	
$\bar{\sigma}_{rr}^{(tot)}$	362.1		90.2		1.159	

cannot limit by any fixed value of n without regard for the remainder of an infinite series after the *n-th* term. There are a number of ways to do this [20]. The simplest method is the summation using the semiclassical Kramers formula which can be written as follows

$$\sum_{n=n'}^{\infty} \sigma_{rr}^{(n)} \propto \sum_{n=n'}^{\infty} \frac{1}{n^3} \frac{Z_{eff}^4}{(E-\epsilon_n)E}, \tag{6}$$

where $\epsilon_n = Z^2/(2n^2)$, $Z_{eff} = Z - N/2$. The quantum defect method gives a more accurate value of $\sum_{n=n'}^{\infty} \sigma_{rr}^{(n)}$. Besides, there are a number of modifications of the methods. We intend to consider available methods of allowing for the rest terms and to adopt the most optimal one in our calculations. For the moment, we estimated the remainder roughly by the use of the Kramers summation. The correction obtained is equal $\sim 4\%$. Net results $\bar{\sigma}_{rr}^{tot}$ are listed in the last line of Table 1. For $E = 1\,\mathrm{keV}$ our result value $\bar{\sigma}_{rr}^{tot} = 90.2\,\mathrm{barn}$ is in good agreement with the corresponding value $\bar{\sigma}_{rr}^{tot} = 90\,\mathrm{barn}$ obtained by Kim and Pratt [20] where the fully relativistic calculations were carried out up to $n = 6$ and the quantum defect method for estimation of the remainder was used.

Table 1 shows also that contribution $\sigma_{rr}^{(n)}$ decreases more rapidly with n for low energy E. For example, the "inner" $3d$ shell contributes 50% at E=0.5 keV, 32% at E=1 keV, and only 2.3% at E=10 keV. On the contrary, the higher 6ℓ shells, for instance, contribute 5.3% at E=0.5 keV, 7.3% at E=1 keV, and 10% at E=10 keV. Most likely, this is due to the different overlapping between the discrete and continuum electron wave functions. This effect may be considered in more detail in future work.

Presented in Table 2 are contributions $\sigma_{rr}^{(\ell)}$ of shells with ℓ = 0,1,2,3,4,5... to $\sigma_{rr}^{(tot)}$. The contribution can be written as

$$\sigma_{rr}^{(\ell)} \;=\; \sum_{n=3}^{15} \sum_{\substack{\kappa=\ell,\\ -(\ell+1)}} \sigma_{rr}^{(n\kappa)}. \tag{7}$$

Table 2: Partial RR cross sections $\sigma_{rr}^{(\ell)}$ (in barn) for ion Fe^{8+}:[Ar] and its contributions to the RR total cross section $\sigma_{rr}^{(tot)}$ $\Delta_\ell = (\sigma_{rr}^{(\ell)}/\sigma_{rr}^{(tot)}) \times 100\%$.

		$E = 0.5$ keV		$E = 1$ keV		$E = 10$ keV	
ℓ	κ	$\sigma_{rr}^{(\ell)}$	$\Delta_\ell, \%$	$\sigma_{rr}^{(\ell)}$	$\Delta_\ell, \%$	$\sigma_{rr}^{(\ell)}$	$\Delta_\ell, \%$
s	–1	23.0	6.6	11.8	14	0.695	62
p	+1,–2	78.7	22	32.0	37	0.372	34
d	+2,–3	241.5	70	42.4	49	0.0429	4
f	+3,–4	4.04	1.2	0.39	0.4	0.000558	0.05
g	+4,–5	0.113	0.02	0.021	0.01	0.000357	0.03
i	+5,–6	0.042	0.01	0.013	0.01	0.000281	0.02
h	+6,–7	0.032	0.01	0.009	0.01	0.000164	0.01
$\sigma_{rr}^{(tot)}$		347.3		86.5		1.112	

As distinct from the data of Table 1, one can note a rapid convergence over ℓ. For example, the contribution of the g-electrons ($\ell = 4$) is $\leq 0.03\%$. Taking into account the rapid convergence and a finite number of terms with various κ, one can ignore terms with $\ell > 4$. This results in the error $\sim 0.1\%$ for the the energy $E = 10$ keV according to the rough assessment.

Besides, also in contrast to contributions $\sigma_{rr}^{(n)}$, we can see that the contribution of atomic shells with the smallest ℓ increases with energy. For example, the s shells contribute 6.6% at E=0.5 keV, 14% at E=1 keV, and 62% at E=10 keV. We assume to consider this phenomenon at length also.

4 Analytic fits

The next problem of our proposal is concerned with the fitting the calculated cross sections by analytic expressions. This problem is assumed to be attacked using the method suggested in our papers [8, 9]. The method is based on the approximate criterion of similarity of PCS for shells with the same n and ℓ for different atoms and ions described by Kamrukov *et al.* (1983) [21]

$$\sigma_{ph}^{nl}(E) = \sigma_0 F(y) \ , \qquad y = E/E_0 \ . \tag{8}$$

Here $\sigma_0 = \sigma_0(nl, Z, N)$ and $E_0 = E_0(nl, Z, N)$ are fitting parameters and $F(y)$ is a "nearly universal" function for all species (Z, N) at a fixed shell nl. According to Eq. (8), in the logarithmic variables $(\log\sigma, \log E)$, each cross section curve can be shifted to the "nearly universal" curve $\log F$. Fig. 4 demonstrates this for the $3s$ and $3p$ shells. A shift along the energy axis is determined by the fit

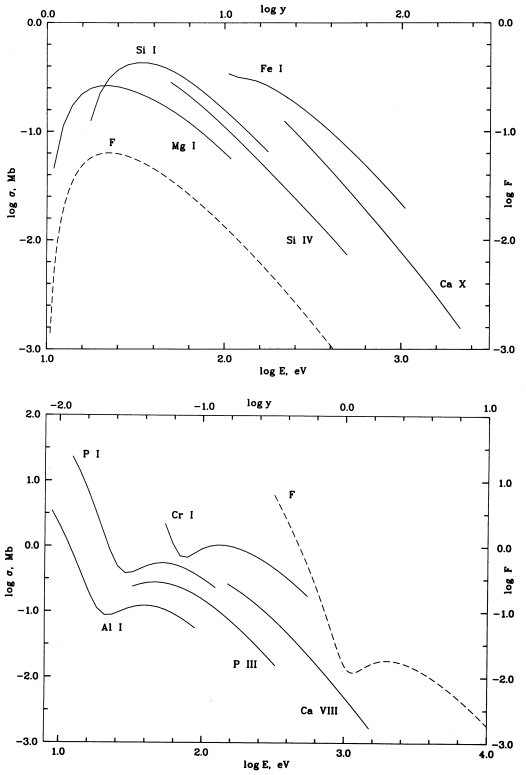

Figure 4: Dirac–Fock–Slater $3s$-shell (top) and $3p$-shell (bottom) PCS $\sigma_{ph}(E)$ for some atoms and ions (solid) and the function $F(y)$ (dashed) from Eq. (9) for the parameters $y_w = 0$, $y_a = 180$, $P = 4.2$ (top) and $y_w = 0.26$, $y_a = 18$, $P = 7.2$(bottom).

parameter E_0 while a shift along the cross section axis by the parameter σ_0. The procedure is successful if an adequate form of $F(y)$ has been figured out.

We found that all cross sections for the ground states are accurately fitted by Eq. (8) with a function $F(y)$ in the following form

$$F(y) = \left[(y-1)^2 + y_w^2\right] y^{-Q} \left(1 + \sqrt{y/y_a}\right)^{-P}, \quad Q = 5.5 + \ell - 0.5P\,. \qquad (9)$$

Here y_w, y_a, and P are three additional fit parameters which depend on the quantum numbers $n\ell$ of the shell under consideration, atomic number Z, and the number of electrons N. The parameters y_w, y_a, and P vary with Z and N but much more slowly than two main parameters σ_0 and E_0. This fact lets us to consider $F(y)$ as "nearly universal". The parameter Q in Eq.(9) is chosen in such a way as to satisfy the well-known nonrelativistic asymptotic behavior $\sigma_{ph}^{(nl)}(E) \propto E^{-3.5-\ell}$ for high energies ($E \to \infty$).

Let us emphasize that each of the five fit parameters in Eqs.(8) and (9) has a simple meaning. Indeed, the PCS curve given by Eqs. (8) and (9) looks different in three energy ranges. For low energies $E \sim E_0$, the cross section for the ground state usually shows a resonance-like minimum. The minimum is located at $E \approx E_0$, and the minimum cross section is determined by y_w. For higher energies $E_0 \ll E \ll E_0 y_a$ (usually we have $y_a \gg 1$), the cross section follows a power law: $\sigma_{ph}^{(nl)}(E) \propto E^{-b}$ and the power-law index is determined by the fit parameter P: $b = 3.5 + \ell - 0.5P$. The high-energy boundary of this energy range is defined by the fit parameter y_a. Finally, at higher energies $E \gg E_0 y_a$, the standard asymptotic behavior $\sigma_{ph}^{(nl)}(E) \propto E^{-3.5-\ell}$ is reproduced. Note that Eqs.(8) and (9) define a real cross section at $E \geq \varepsilon$. For outer shells of neutral or low-ionized atoms one usually has $\varepsilon \sim E_0$, and the cross section minimum is actually or partially realized. For any shells of highly ionized atoms and for inner shells of low-ionized ones, one has $\varepsilon \gg E_0$. In these cases, the minimum is not realized and the actual cross section decreases monotonously with E. Note also that if y_w is rather large, the minimum of $\sigma_{ph}^{(nl)}(E)$ at $E \sim E_0$ disappears, and Eqs.(8) and (9) predict monotonous decreasing of PCS with E at any E. The fit parameters were determined by minimizing the mean-square relative deviation from calculated PCS.

The accuracy of fitting for inner and outer shells of a number of neutral atoms is demonstrated in Figs. 5 and 6 which are taken from our paper [9]. We can see that fitting curves reproduce PCS calculations performed by the Dirac–Fock–Slater method (dark circles) with a good accuracy. It should be noted that presented in Fig. 6 are the worst cases.

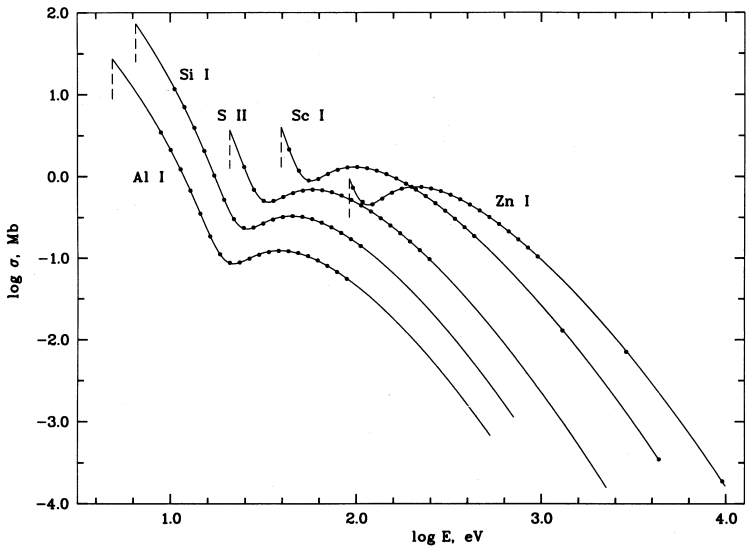

Figure 5: Calculated (•) and fitted (solid) $3p$-shell PCS some atoms and ions.

Fig. 7 shows the comparison of fitting curves and PCS values obtained in the framework of the Dirac–Fock method for the ion Fe^{7+}. The $3d$, $4s$, $4p$, $4d$, and $4f$ excited states are presented. One can see the excellent agreement in calculated and fitted values in all cases.

Consequently, the description by the use of Eqs. (8) and (9) is accurate enough for ground and low-excited states. High-excited states are likely to be fitted by more simple expressions with less number of fit parameters. This is also the problem of future studies.

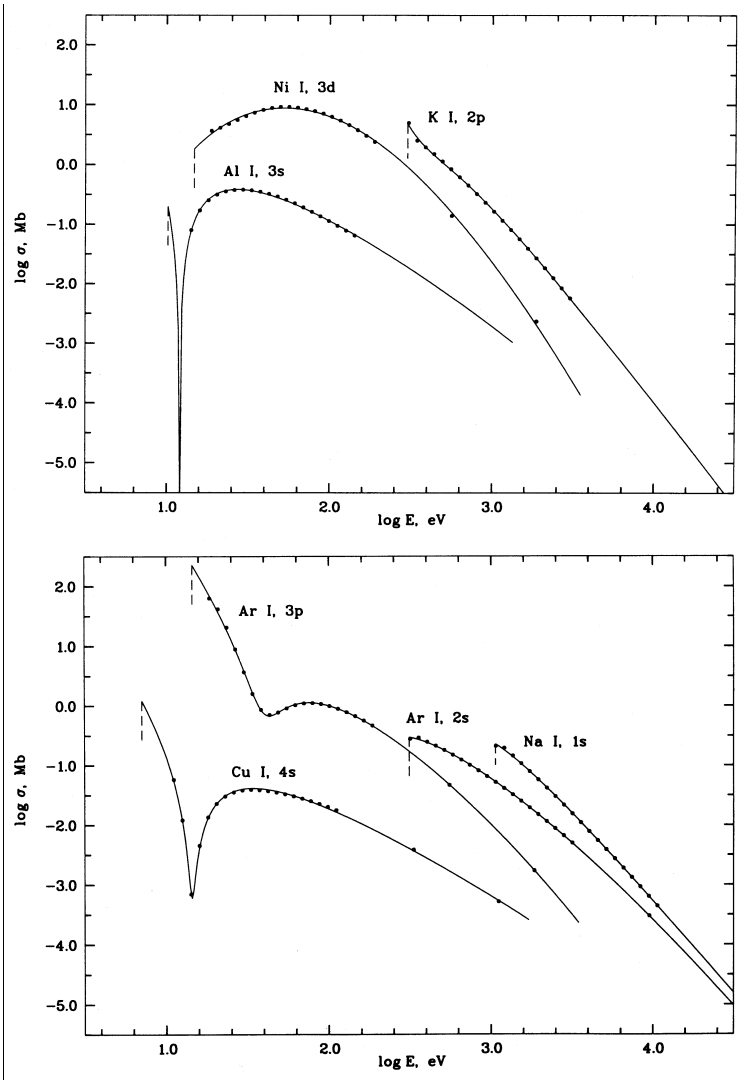

Figure 6: Calculated (•) and fitted (solid) subshell PCS for the worst-fitting cases.

5 Work plan for first two years

In the first year we intend to performed the following points.

1) The available data for RR and photoionization processes will be analyzed to identify the specific heavy element impurity ions for which data are of a prime necessity in the study of plasma modeling and in diagnostics.

2)Relativistic calculations of the subshell photoionization and RR cross sections will be carried out in the framework of the Dirac-Fock method for ground and excited states of some heavy element impurities from neutrals to highly charged ions.

3) The method of an estimation of the remainder of the infinite series which

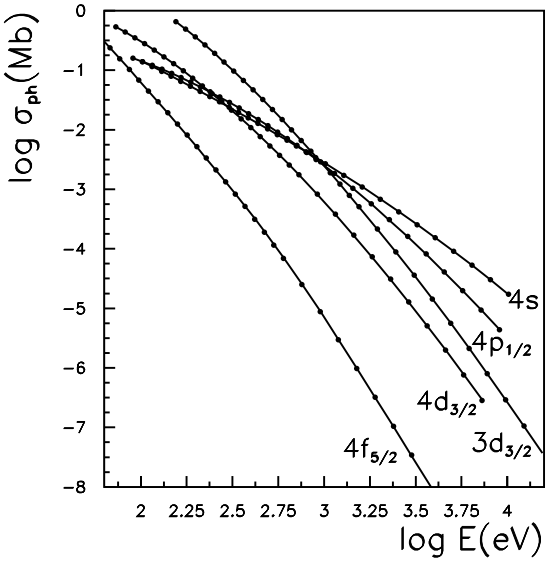

Figure 7: Calculated (•) and fitted (solid) subshell photoionization cross sections for different $n\ell j$ shells of the ion Fe^{7+}:[Ar]$n\ell j$.

is best suited to our calculations of the total RR cross section will be adopted.

4) The fitting procedure used previously for ground states of rather light elements will be verified and refined to describe accurately the PCS/RR cross sections of ground and excited states of heavy atoms and ions.

References

[1] M.J. Seaton. *Atomic data for opacity calculations: I General description.* J. Phys. B **20**, 6363 (1987).

[2] J.A. Fernley, A. Hibbert, A.E. Kingston and M.J. Seaton. *Atomic data for opacity calculations: XXIV. The boron-like sequence.* J. Phys B **32**, 5507 (1999).

[3] Robert E.H. Clark, Robert D. Cowan and Frank W. Bobrowicz. *Isoelectronic sequence fits to configuration-average photoionization cross sections and ionization energies.* Atomic Data and Nuclear Data Tables **34**, 415 (1986).

[4] A. Ichihara and J. Eichler. *Cross sections for radiative recombination and the photoelectric effect in the K, L, and M shells of one-electron systems with 1≤ Z ≤112 calculated within an exact relativistic description.* Atomic Data and Nuclear Data Tables **74**, 1 (2000).

[5] Sultana N. Nahar and Antil K. Pradhan. *Self-consistent R-matrix approach to photoionization and unified electron-ion recombination.* Radiation Physics and Chemistry **70**, 323-344 (2004).

[6] M.B. Trzhaskovskaya and V.K. Nikulin. *Radiative recombination of an electron with multiply charged uranium ions.* Optics and Spectroscopy **95**, 537 (2003).

[7] G. Bednarz, A. Warczak, D. Sierpowski *et al.*, GSI Sci. Rep. 2000, p.90

[8] I.M. Band, M.B. Trzhaskovskaya, D.A. Verner and D.G. Yakovlev. *K-shell photoionization cross sections: calculations and simple fitting formulae.* Astron. Astrophys. **237**, 267 (1990).

[9] D.A. Verner, D.G. Yakovlev, I.M. Band and M.B. Trzhaskovskaya. *Subshell photoionization cross sections and ionization energies of atoms and ions from He to Zn.* Atomic Data and Nuclear Data Tables **55**, 233 (1993).

[10] I.M. Band, Yu.I. Kharitonov and M.B. Trzhaskovskaya. *Photoionization cross sections and photoelectron angular distributions.* Atomic Data and Nuclear Data Tables **23**, 443 (1979).

[11] M.B. Trzhaskovskaya, V.I. Nefedov and V.G. Yarzhemsky. *Photoelectron angular distribution parameters for elements Z=1 to Z=54 in the photoelectron energy range 100–5000 eV.* Atomic Data and Nuclear Data Tables **77**, 97, 2001; *ibid.: Photoelectron angular distribution parameters for elements Z=55 to Z=100 in the photoelectron energy range* 100–5000 eV. **82**, 257, 2002.

[12] M.B. Trzhaskovskaya, V.K. Nikulin, V.I. Nefedov and V.G. Yarzhemsky. *Relativistic photoelectron angular distribution parameters in quadrupole approximation.* J. Phys. B **34**, 3221 (2001).

[13] M.B. Trzhaskovskaya, V.K. Nikulin, V.I. Nefedov and V.G. Yarzhemsky. *Influence of nondipolar effects on the photoelectron angular distribution in photoionization of the 2p and 3d atomic shells.* Optics and Spectroscopy **96**, 765 (2004).

[14] M.B. Trzhaskovskaya, V.K. Nikulin, V.I. Nefedov and V.G. Yarzhemsky. *Nondipolar second order parameters of photoelectron angular distribution for elements Z=1 to Z=100 in the photoelectron energy range 1–10* keV. Atomic Data and Nuclear Data Tables (2005, in print).

[15] M.B. Trzhaskovskaya, V.I. Nefedov and V.K. Nikulin. *Multipole effects in angular distribution of photoelectrons.* Optics and Spectroscopy **91**, 594 (2001).

[16] I.M. Band, M.A. Listengarten, M.B. Trzhaskovskaya and V.I. Fomichev. *Computer program complex RAINE*, I–YI, Leningrad Nuclear Physics Institute Reports, LNPI-289 (1976), LNPI-298, 299, 300 (1977), LNPI-498 (1979), LNPI-1479(1989).

[17] G.C. Angel and James A.R. Sampson. *Total photoionization cross sections of atomic oxygen from threshold to 44.3 A-ring* Phys.Rev. **A38**, 5578 (1988).

[18] J.A.R. Samson, L. Lyn, G.N. Haddad, and G.C. Angel. J. Phys. IV (Colloq.) **1**, C1-99 (1991).

[19] B.L. Henke, P. Lee, T.J. Tanaka, R.L.Shimabukuro, and B.K. Fujikawa. *Low energy X-ray interaction coefficients: photoabsorption, scattering and reflection.* Atomic Data and Nuclear Data Tables **27**, 1 (1982).

[20] Young Soon Kim and R.H. Pratt. *Direct radiative recombination of electrons with atomic ions:cross sections and rate coefficients*. Phys. Rev. **27**, 2913 (1983).

[21] A.S. Kamrukov, N.P. Kozlov, Yu.S. Protasov, and S.N. Chuvashev. *On the calculation of photoionization cross section spectra of non-hydrogen-like atoms and ions*. Opt. Spectroscopy **55**, 17 (1983).